



SCIREA Journal of Materials

<http://www.scirea.org/journal/Materials>

June 24, 2022

Volume 7, Issue 2, April 2022

<https://doi.org/10.54647/materials43184>

## CaP Precipitation on Titanium under UV Lighting and Effect of Urea Concentration

Qing Zhou\*, Liang-Liang Zhang, Ming-Li Xie

College of Mechanical and Electrical Engineering, Nanjing University of Aeronautics and Astronautics, Nanjing, China

\*Corresponding author: [anzhouqing@nuaa.edu.cn](mailto:anzhouqing@nuaa.edu.cn)

### Abstract

This paper reports the precipitation of calcium phosphate (CaP) on alkaline hydrothermally treated titanium alloy under ultraviolet (UV) lighting. Urea ( $\text{NH}_2\text{CONH}_2$ ) with different concentrations were added into a simulated body fluid buffered by sodium lactate.  $\text{CO}_2$  and  $\text{NH}_3$  gas release during immersion tests were detected. The pH values were also examined during the tests. The results show that the detected  $\text{NH}_3$  and  $\text{CO}_2$  concentrations near the solution are larger than those in the air. The release of  $\text{NH}_3$  and  $\text{CO}_2$  due to the hydrolysis of urea was confirmed both under UV lighting and under dark. It is shown by SEM photographs that the precipitated CaP particles are surrounded by organic which is supposed to be lactate deposition after 14 days immersion. A structure of embedded CaP particles in organic deposition matrix is considered as a primary stage of the formation of CaP-CO-NaCl layer. UV lighting causes the contents of Na and Cl increased, but C and O decreased.

**Keywords:** *CaP biomineralization, photocatalysis,  $\text{NH}_3$  release,  $\text{CO}_2$  release, urea, titanium alloy*

## 1. Introduction

Titanium and titanium alloy are used as biomaterials in the fields of hard tissue substitute, dental implant et al due to their higher mechanical properties and biocompatibility [1]. To improve their surface bioactivity other authors have proposed a method of manufacturing hydroxyapatite (HA) layer on titanium [2,3,4]. HA is proposed to promote osteoblast cell proliferation and growth [5,6]. Although the presentative of HA is a crystalline in the form of  $\text{Ca}_{10}(\text{PO}_4)_6(\text{OH})_2$  the existence in actual bone at different developing periods and different tissues do not have this format [7]. Amorphous phase or a combination of crystalline and non-crystalline and the presence of Cl, F,  $\text{CO}_3$  were found [7]. Ca sometime is substituted by Mg, Zn or Na. Other authors [8,9,10] call the series compounds calcium phosphate (CaP).

The effect of  $\text{TiO}_2$  photocatalysis on CaP formation has been investigated in the papers [11-13]. It is known that  $\text{TiO}_2$  existing in the states of anatase and rutile has excellent photocatalysis [14]. The photocatalysis is supposed to be produced by photo-induced electrons and holes separation at the surface of  $\text{TiO}_2$ , and causing redox reaction [15]. Photoactivated water molecular splitting is also considered as a source [16]. An acceleration effect of CaP formation photoactivated by ultraviolet (UV) lighting was reported [11,13]. The shape and the crystallinity of CaP, which influence the bioactivity and dissolution rate of CaP [17] may be altered by photocatalysis.

Urea is an existence in blood plasma and a metabolic result of protein in human body. There are several exploratory studies [18-20] synthesizing HA powder from urea added physiological solutions. In this work, in vitro CaP formation under photocatalysis by using a urea added simulated body solution (SBF) is investigated.

## 2. Experimentals

The experimental procedures include  $\text{TiO}_2$  layer preparation on titanium alloy by alkaline hydrothermal method, immersion tests in a SBF under UV lighting and the CaP precipitation observation and composition analysis.

### 2.1. $\text{TiO}_2$ Layer Preparation on Titanium Alloy

Titanium alloy (Ti-6Al-4V) bars were purchased commercially (BaoTi, Co., Baoji, China). A piece with the size of  $\phi 16\text{mm} \times 3\text{mm}$  was obtained by wire-cutting. The surfaces of pieces were ground with 400-1500# abrasive papers gradually. Then they were polished with

alumina powder (1.5  $\mu\text{m}$ ). They were cleaned in ethanol and deionized water 15 min under ultrasonic vibration progressively.

Alkaline hydrothermal treatment of the titanium surface was according to the method proposed by Peng [21]. The titanium alloy pieces were put into a stainless-steel autoclave with 2.5 M NaOH (GR >98.0%, Nanjing Chemical reagent Co., China) solution. The autoclave has a Teflon inner container which is corrosion-resistant. Then the autoclave was heated to 150°C and kept for 15 hours. After the pieces were cooled to the room temperature with the oven, the titanium pieces were then immersed in deionized water for 3 days. They were then immersed in 1 M HNO<sub>3</sub> solution (diluted from 60wt% HNO<sub>3</sub>, Shanghai Pilot Chemical Industry, China) for 3 days, cleaned and dried, and finally annealed in an electric furnace at 600°C for 5 hours in air.

## 2.2. Immersion Tests

The solution used in the immersion tests was an SBF with the compositions of Na<sup>+</sup> 142, Cl<sup>-</sup> 103, Ca<sup>2+</sup> 2.5, Mg<sup>2+</sup> 1.5, HPO<sub>4</sub><sup>2-</sup> 1, HCO<sub>3</sub><sup>-</sup> 27, SO<sub>4</sub><sup>2-</sup> 0.5, K<sup>+</sup> 5mM, which are near those of human blood. The SBF were made by adding NaCl 5.26, CaCl<sub>2</sub>·2H<sub>2</sub>O 0.368, Na<sub>2</sub>HPO<sub>4</sub>·2H<sub>2</sub>O 0.178, KCl 0.373, NaHCO<sub>3</sub> 2.268, MgCl<sub>2</sub>·6H<sub>2</sub>O 0.305, Na<sub>2</sub>SO<sub>4</sub> 0.071g/L (all GR level purity, Shanghai Aladdin Co., China) into deionized water. Sodium L-lactate (60% aqueous solution, Shanghai Aladdin Co., China) was used as buffer reagent. Use L-lactic acid (90%, Shanghai Aladdin Co., China) for pH adjustment to 7.4. Lactate acid is one of the metabolic results of human body [22]. The solution was filtered by a 0.2 $\mu\text{m}$  filter head. Then 2, 10 and 30mM urea (99.5%, Shanghai Aladdin Co., China) was added into the SBF separately.

Immersion tests of the hydrothermally treated pieces under UV lighting were carried out in a 37°C water bath. An Hg ultraviolet lamp (18W GPH303T5L, Kadind, USA) was hung over the liquid level 150mm. A quartz glass piece was covered on the dish for preventing dust and bacteria from entering into the solution while allowing UV light transmission. For UV lighting details refer to our previous work [23]. A UV radiation flux meter (SDR2040, 250~410nm wavelength UV probe, Shenzhen Speedre Co., China) was used to probe the radiation flux of UV behind the quartz glass piece and 150mm far away from the lamp. A maximum radiation flux of 4.2mW/cm<sup>2</sup> was obtained.

An irradiation pattern of 4 hours lighting and 20 hours dark was applied per day and lasted 14 days. Immersion tests under a total dark environment were also carried out for comparison. The releases of CO<sub>2</sub> and NH<sub>3</sub> gases during immersion were detected by a NDIR CO<sub>2</sub>

transmitter and a NH<sub>3</sub> sensor (VMS 3002-CO<sub>2</sub>, NH<sub>3</sub>, Shangdong Vemsee Tech. Co., Jinan, China), respectively. The values of pH of the solution during immersion were examined by a pH meter (PHS-3C, INESA Instrument, Shanghai, China).

### 2.3. SEM and EDS

Immersed surfaces of titanium pieces were observed by a scanning electronic microscopy (SEM, JSM-6360LV JEOL, Tokyo Japan). The compositions of the interesting areas were probed by an energy dispersive spectroscopy (EDS, 2000XMS60, GENESIS) attached to the SEM.

## 3. Results and Discussion

### 3.1. NH<sub>3</sub> and CO<sub>2</sub> emission

During the immersion of the pieces in the urea added SBF the occurrence of NH<sub>3</sub> and CO<sub>2</sub> gas releases is because of the reaction of urea with water. The hydrolysis of urea is expressed by the follow [18],



**Table 1. NH<sub>3</sub> release during immersion of titanium pieces in urea added SBF.**

Soaking time (h)	NH <sub>3</sub> (ppm)						
	U2	U10	U30	D2	D10	D30	In air
4	12	13	12	19	23	24	7
28	16	18	17	21	18	22	14
52	33	35	35	39	37	42	22
76	21	19	20	19	20	20	11
100	23	24	26	27	30	31	18
124	13	14	16	15	16	17	11
148	12	12	13	14	15	13	8
172	10	12	14	11	12	11	8

196	15	18	18	19	17	19	12
220	12	14	15	20	19	19	9
244	9	11	11	13	12	15	7
268	17	20	21	20	22	22	11
292	25	29	28	29	28	31	11
316	31	29	30	32	31	32	17

Equation (1) can be accelerated with the help of catalysis [18] although it also occurs at room temperature without catalysis. Table 1 and Table 2 list the detected  $\text{NH}_3$  and  $\text{CO}_2$  gas concentrations in ppm near the solution surfaces, respectively. U2, U10 and U30 denote the samples immersed in the SBF with urea concentration of 2, 10, 30mM under UV lighting, respectively. D2, D10 and D30 denote the samples immersed in the SBF with urea concentration of 2, 10, 30mM under dark, respectively. The gas concentrations in the air at room temperature within the lab room were also probed during the soaking time and listed in Table 1 and 2, too. Corresponded figures are shown in Figure 1 and 2.

**Table 2.  $\text{CO}_2$  release during immersion of titanium pieces in urea added SBF.**

Soaking time (h)	$\text{CO}_2$ (ppm)					
	U10	U30	D2	D10	D30	In air
4	629	618	622	631	638	518
28	1260	1264	1225	1215	1214	957
52	1222	1288	927	945	1003	974
76	717	705	739	722	699	620
100	1080	1028	1138	1123	1149	877
124	856	817	792	765	758	580
148	881	814	908	866	870	587
172	817	862	784	864	625	528
196	604	586	544	560	543	521

220	747	687	567	574	558	461
244	741	686	651	644	631	563
268	958	785	774	745	773	493
292	733	677	697	729	708	497
316	873	715	713	693	676	604

It is noted that the NH<sub>3</sub> and CO<sub>2</sub> gas concentrations change with the soaking time for all the samples. They are all more than those of the concentrations in air, indicating continuous release of these two kinds of gases from the solution. NH<sub>3</sub> released from urea is water soluble. The ionization of NH<sub>3</sub> · H<sub>2</sub>O is expressed by,



Because Equation (2) is reversible, it is possible NH<sub>3</sub> releases under the condition that the reverse process is predominated, for an example, the increase in OH<sup>-</sup>.

The solubility of CO<sub>2</sub> in water is limited (0.1g/100g=CO<sub>2</sub>/water at 37°C [24]). The dissolution of CO<sub>2</sub> into water is expressed in the follows,



From Equation (4) more CO<sub>3</sub><sup>2-</sup> production can be obtained with the increase of OH<sup>-</sup>, i.e. the decrease of H<sup>+</sup> and pH increment. The CO<sub>3</sub><sup>2-</sup> is a component of carbonated CaP, for example, Ca<sub>10</sub>(PO<sub>4</sub>)<sub>6</sub>CO<sub>3</sub> [24]. The necessary amount of CO<sub>3</sub><sup>2-</sup> for forming carbonated CaP deposition is low because of the lower solubility of carbonated CaP [24].

It can be seen from Figure 1 and 2 that there is sharp increase of NH<sub>3</sub> and CO<sub>2</sub> release in the initial immersion stage. The release of CO<sub>2</sub> is faster than that of NH<sub>3</sub> which may be due to much lower solubility of CO<sub>2</sub> compared to NH<sub>3</sub>. Slightly larger NH<sub>3</sub> release under dark than under UV lighting but less CO<sub>2</sub> under dark than under UV lighting can be confirmed as shown in Figure 1 and 2. It indicates the UV lighting inhibits NH<sub>3</sub> release but promotes CO<sub>2</sub> release. More CO<sub>2</sub> release under UV lighting is agreeable to the decreased carbon content in the carbonated CaP formed under UV lighting as showing in the results of EDS (Table 3)

It can be observed in Figure 1 that slightly increased release of NH<sub>3</sub> as the urea concentration is increased. This is because the source of NH<sub>3</sub> is only from urea. However, the release of

CO<sub>2</sub> (Figure 2) seems to be suppressed due to the urea addition particularly after 200h immersion under UV lighting. The reason may be due to that more urea causes the increase of free NH<sub>4</sub><sup>+</sup> and OH<sup>-</sup> according to Eq (2) and less CO<sub>2</sub> according to Equation (3) and (4).

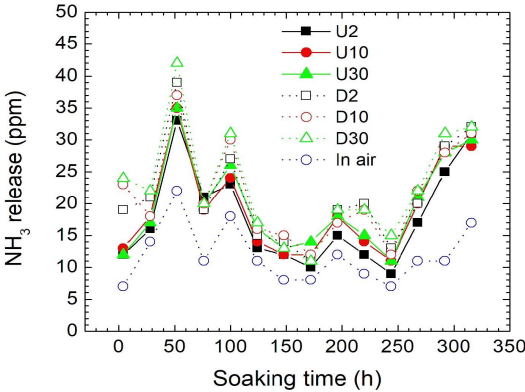


Figure 1. NH<sub>3</sub> release amounts probed at the places near the solution surfaces during immersion.

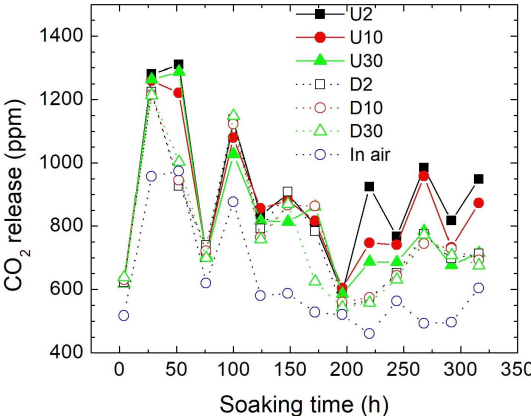


Figure 2. CO<sub>2</sub> release amounts probed at the places near the solution surfaces during immersion.

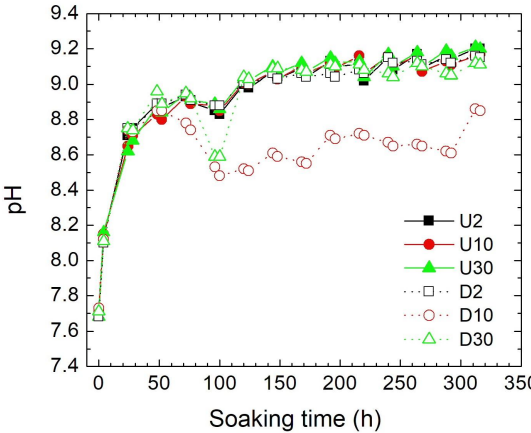
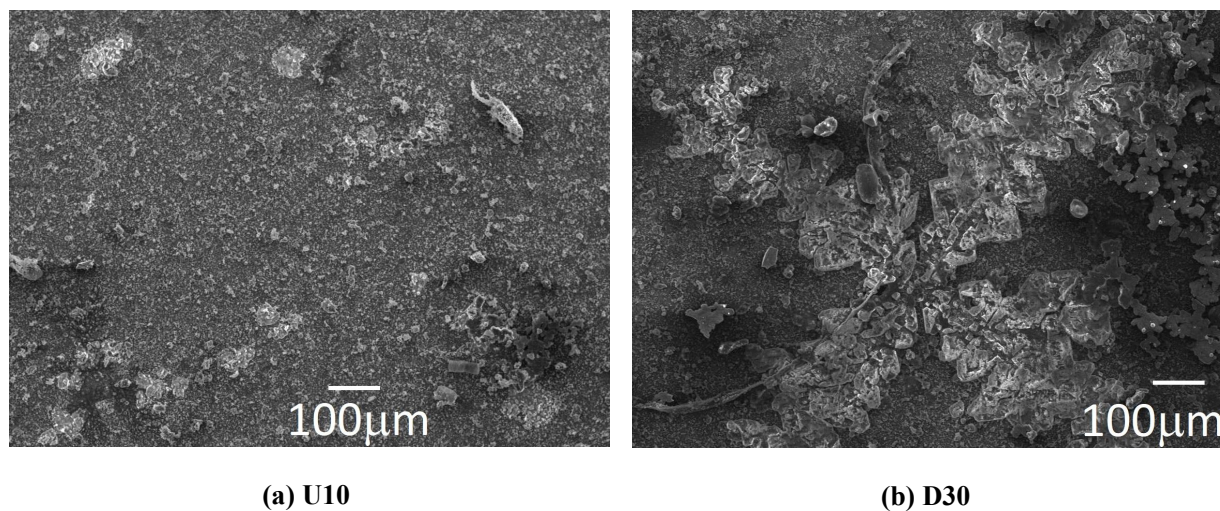


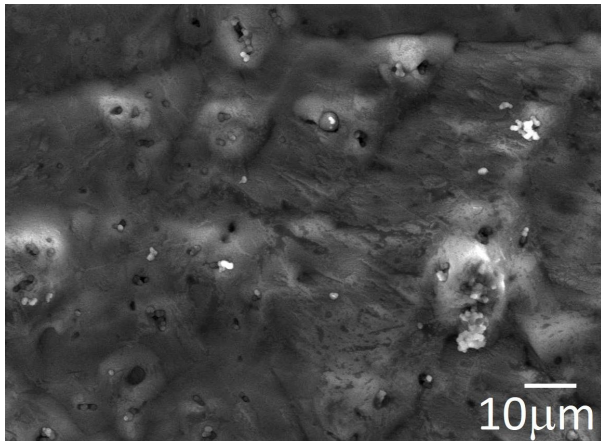
Figure 3. Values of pH of the solution during immersion.

Figure 3 shows the pH plots against the soaking time. The increase of pH is fast at the initial stage (1-2 days), a slow increase stage is followed until the end of test. A pH decrease trend is seen for the D10 samples after 50 hours, the reason of which is unknown. Indifferent pH values evolution can be observed due to the urea concentration effect.

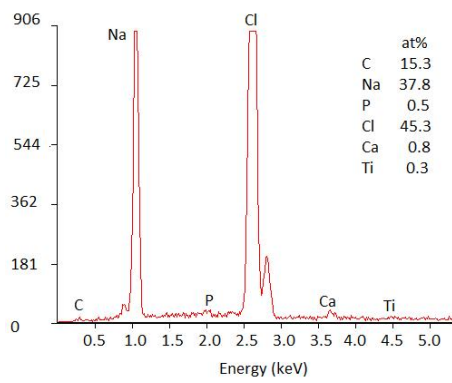
### 3.2. Surface Morphology and Composition

The results of the SEM observation of the surfaces after the immersion tests are shown in Figure 4. Different distributions of white particles areas between the U10 and D30 samples: isolated islands on U10 and dendritic shape on D30 are shown (Figure 4a and 4b, 4c and 4d). Such different morphologies were also observed on U2, U30, D2 samples. The dendritic shaped area detected by an EDS analysis (Figure 4f) is mainly composed of Na, Cl, C, O elements and small quantities of K, Ca, Ti and P elements. But the compositions of isolated islands mainly are Na, Cl, C, and small amounts of Ca, Ti and P (Figure 4e). It can be seen the white particles areas are composed of CaP particles and crystallized NaCl surrounding including C-O organic deposition. The existence of C in the crystalline under UV lighting and C-O under dark is interesting. The white CaP particles dotted crystallized NaCl-C surrounding can be seen on Figure 4c, but the CaP particles formed under dark are aggregated, NaCl crystal and organic (rectangular area) are formed separately (Figure 4d).

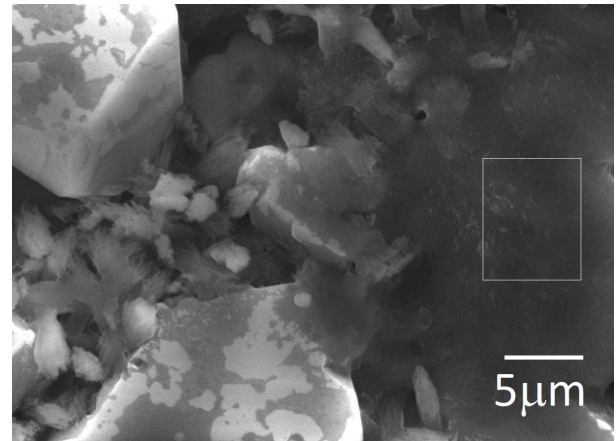




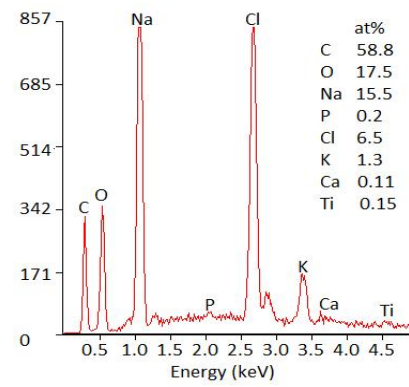
(c) U10



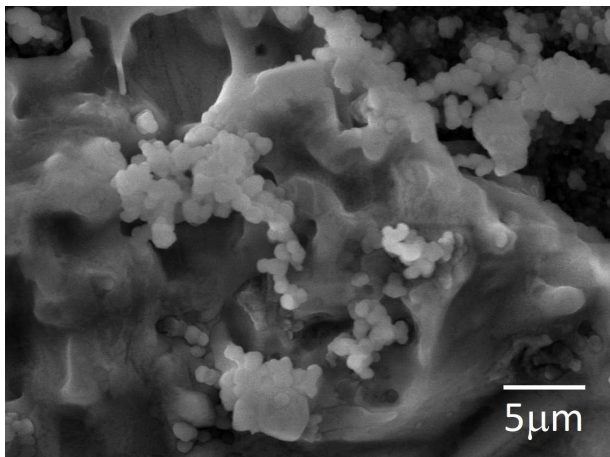
(e) U10



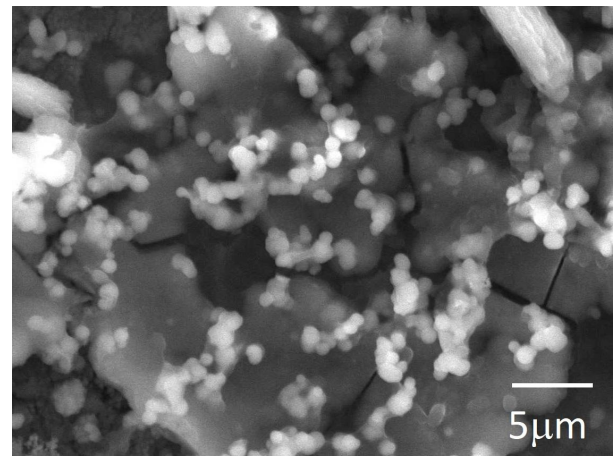
(d) D30



(f) D30



(g) U10



(h) D10

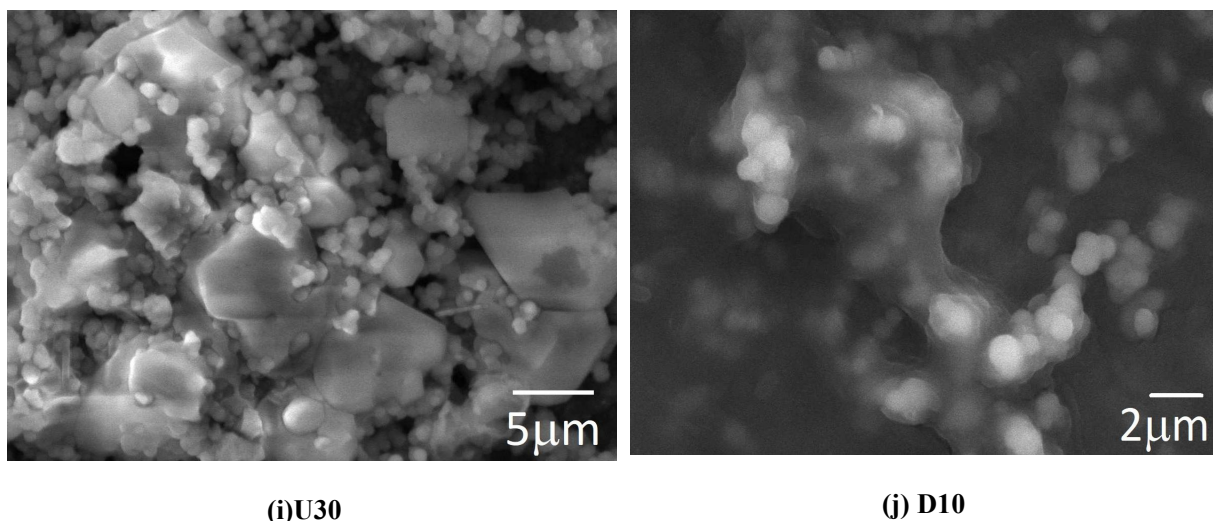


**Figure 4. SEM observation of the surface morphologies of hydrothermally treated titanium alloy pieces after immersion tests in simulated body fluid containing urea. (a, c, g) U10, (i) U30, (b, d) D30, (e, f) corresponded EDS of (c) and the rectangular in (d), (h, j) D10.**

More SEM photographs (Figure 4g and 4i) show CaP particles formed under UV lighting are surrounded by NaCl-C-O crystal. How the bond of C-O being connected with NaCl crystal needs more studies. We can see CaP particles embedded in C-O organic (Figure 4j). The C-O organic is supposed to be produced from lactate deposition. The organic includes Na and Cl elements obtained by EDS results (Table 3), but the contents of Na and Cl formed under UV lighting is increased largely compared to those under dark. Compared to the organic matter formed under dark, more crystals are formed under UV irradiation.

Table 3 lists the compositions of the elements in the deposition, it can be seen that less C and O, but more Na and Cl in the CaP particles on U series samples than D series samples. The contents of Ca and P are almost similar for U and D series samples, Mg, Na, K, Cl, Ti elements are included in the CaP particles. No nitrogen is found on the surfaces. It is supposed that nitrogen exists in the form of  $\text{NH}_4^+$  and is released with the emission of  $\text{NH}_3$ . The ratios of Ca/P are ranged in 1.61~1.64 under UV lighting, 1.31~1.53 under dark. The Ca/P of U series samples are bigger than those of D series.  $\text{Ca}_6(\text{PO}_4)_{10}\text{CO}_3$  formation is supposed due to the Ca/P ratio of near 1.6 and  $\text{NH}_3$  gas release.  $\text{OH}^-$  ion in the solution is increased with the soaking time according to Equation (2) until the  $\text{NH}_3$  gas releases. Consequently no  $\text{OH}^-$  can be involved into the formation of  $\text{Ca}_6(\text{PO}_4)_{10}(\text{OH})_2$ .

**Table 3. Compositions of the precipitated CaP (white particles in SEM) detected by EDS (at%)**

	C	O	Na	Mg	K	Cl	Ti	P	Ca	Ca/P
U2	43.9	13.5	11.5	1.4	0.9	15.2	0.2	4.9	7.9	1.61
U10	35.9	15.6	14.6	1.4	3.3	14.0	0.2	4.8	7.9	1.64
U30	34.0	11.4	16.9	1.0	0.3	25.0	0.6	4.1	6.7	1.63
D2	50.0	17.9	7.5	1.9	0.5	6.6	2.6	5.1	7.8	1.53
D10	60.0	21.1	1.6	1.4	0.2	0.6	0.7	6.2	8.1	1.31
D30	43.1	29.2	4.0	2.2	0.5	0.4	4.8	6.8	9.1	1.34

#### 4. Summary Remarks

An investigation of CaP precipitation on the hydrothermal treated Ti-6Al-4V by immersed in a simulated body fluid with urea addition under UV irradiation was carried out. The SBF used in this work is a sodium lactate and lactic acid buffered solution system. The release of NH<sub>3</sub> and CO<sub>2</sub> during the immersion tests was confirmed in consideration that detected NH<sub>3</sub> and CO<sub>2</sub> concentrations near the surface of the solutions are larger than those in the air. NH<sub>3</sub>: 9-40 ppm, and CO<sub>2</sub>: 543-1264 ppm. The release of two kinds of gases is related to the hydrolysis of NH<sub>2</sub>CONH<sub>2</sub> which occurs both under UV lighting and under dark. NH<sub>3</sub> and CO<sub>2</sub> were first dissolved in the SBF solution, and then released. NH<sub>3</sub> release under UV lighting is slightly less than under dark, but CO<sub>2</sub> release under UV lighting is larger than under dark. Particularly, a larger CO<sub>2</sub> release was observed in the later immersion stage under UV lighting compared to those under dark. It seems UV lighting promotes CO<sub>2</sub> release, but limits NH<sub>3</sub> release.

No significant effect of the urea concentration within the range of 2 ~ 30 mM on CaP precipitation and NH<sub>3</sub> and CO<sub>2</sub> gas release have been observed. However, the photocatalysis caused by UV lighting had large influence on CaP precipitation and the ratio of Ca/P. The ratio of Ca/P near 1.6 and the CaP particles dotted in the crystallized NaCl-C-O matrix were observed on the photocatalytic titanium surfaces. A structure of embedded CaP particles into organic deposition matrix is considered as a primary stage of the formation of CaP-CO-NaCl layer. UV lighting causes the contents of Na and Cl increased, but C and O decreased.

## References

- [1] Shah, F.A.; Trobos, M.; Thomsen, P.; Palmquist, A. Commercially pure titanium (cp-Ti) versus titanium alloy (Ti6Al4V) materials as bone anchored implants - Is one truly better than the other? *Materials Science Engineering C*, 2016, 62, 960-966, doi:10.1016/j.msec.2016.01.032.
- [2] Hayakawa, S.; Okamoto, K.; Yoshioka, T. Accelerated induction of in vitro apatite formation by parallel alignment of hydrothermally oxidized titanium substrates separated by sub-millimeter gaps. *Journal of Asian Ceramic Society*, 2019, 7, 90-100, doi:10.1080/21870764.2019.1572690.
- [3] Posternak, M.; Baldereschi, A.; Delley, B. Adsorption of HPO<sub>x</sub> and CaHPO<sub>x</sub> (x=1,...4) molecules on anatase TiO<sub>2</sub> (001) surfaces. *Surface Science*, 2019, 679, 93-98, doi:10.1016/j.susc.2018.09.002.
- [4] Wu, M.; Wang, T.; Zhang, J.; Qian, H.; Miao, R.; Yang, X. PDA/ CPP bilayer prepared via two-step immersion for accelerating the formation of a crack-free biomimetic hydroxyapatite coating on titanium substrates. *Materials Letter*, 2017, 206, 56-59, doi:10.1016/j.matlet.2017.06.052.
- [5] Kapoor, R.; Sistla, P.G.; Kumar, J.M.; Raj, T.A.; Srinivas, G.; Chakraborty, J.; Sinha, M.K.; Basu, D.; Pande, G. Comparative assessment of structural and biological properties of biomimetically coated hydroxyapatite on alumina ( $\alpha$ -Al<sub>2</sub>O<sub>3</sub>) and titanium (Ti-6Al-4V) alloy substrates. *Journal of Biomedical Materials Research - Part A*, 2010, 94A, 913-926, doi:10.1002/jbm.a.32767
- [6] Zhao, S.F.; Jiang Q.H.; Peel, S.; Wang, X.X.; He, F.M. Effects of magnesium-substituted nanohydroxyapatite coating on implant osseointegration. *Clinical Oral Implants Research*, 2013, 24, 34-41, doi:10.1111/j.1600-0501.2011.02362.x.
- [7] Combes, C.; Cazalbou, S.; Rey, C. Apatite biominerals. *Minerals*, 2016, 6, 1-25, doi:10.3390/min6020034.
- [8] HavitcGlu, H.; Cecen, B.; Pasinli, A.; Yuksel, M.; Aydin, I.; Yildiz, H. In vivo investigation of calcium phosphate coatings on Ti6-Al-4V alloy substrates using lactic acid - sodium lactate buffered synthetic body fluid. *Acta Orthopaedica et Traumatologica Turcica*, 2013, 47, 417-422, doi: 10.3944/AOTT.2013.2885.
- [9] Zhang, L.J.; Liu, H.G.; Feng, X.S.; Zhang, R.J.; Zhang, L.; Mu, Y.D.; Hao, J.C.; Qian, D.J.; Lou, Y.F. Mineralization Mechanism of Calcium Phosphates under Three Kinds of Langmuir Monolayers. *Langmuir*, 2004, 20, 2243-2249, doi:10.1021/la035381j.

- [10] Catauro, M.; Papale, F.; Sapio, L.; Naviglio, S. Biological influence of Ca/P ratio on calcium phosphate coatings by sol-gel processing. *Material Science and Engineering C*, 2016, 65, 188-193, doi:10.1016/j.msec.2016.03.110.
- [11] Chen, M.F.; Zhang, J.; You, C. Ultraviolet-accelerated formation of bone-like apatite on oxidized Ti-24Nb-4Zr-7.9Sn alloy. *Front Materials Science*, 2013, 7, 362-369, doi: 10.1007/s11706-013-0208-6.
- [12] Kawashita, M.; Matsui, N.; Miyazaki, T.; Kanetaka, H. Effect of ammonia or nitric acid treatment on surface structure, in vitro apatite formation, and visible-light photocatalytic activity of bioactive titanium metal. *Colloids Surfaces B Biointerfaces*, 2013, 111, 503-508, doi:10.1016/j.colsurfb.2013.06.049.
- [13] Han, Y.; Xu, K. Photoexcited formation of bone apatite-like coating on micro-arc oxidized titanium. *Journal of Biomedical Materials Research*, 2004, 71, 608-614, doi:10.1002/jbm.a.30177.
- [14] Hanaor, D.A.H.; Sorrell, C.C. Review of the anatase to rutile phase transformation. *Journal of Materials Science*, 2011, 46, 855-874, doi:10.1007/s10853-010-5113-0.
- [15] Schneider, J.; Matsuoka, M.; Takeuchi, M.; Zhang, J.L.; Horiuchi, Y.; Anpo, M.; Bahnemann, D.W. Understanding TiO<sub>2</sub> photocatalysis: Mechanisms and materials. *Chemical Reviews*, 2014, 114, 9919-9986, doi:10.1021/cr5001892.
- [16] Pulpytel, J.; Fakhouri, H.; Smith, W.; Arefi-Khonsari, F.; Meshkini, F. Control of the visible and uv light water splitting and photocatalysis of nitrogen doped tio<sub>2</sub> thin films deposited by reactive magnetron sputtering. *Applied Catalysis B: Environmental*, 2014, 144, 12-21.
- [17] Dal Sasso, G.; Asscher, Y.; Angelini, I.; Nodari, L.; Artioli, G. A universal curve of apatite crystallinity for the assessment of bone integrity and preservation. *Scientific Reports*, 2018, 8, 1-13, doi:10.1038/s41598-018-30642-z.
- [18] Jokic, B.; Tanaskovic, D.; Jankovic-Castvan, I.; Drmanic, S.; Petrovic, R.; Janackovic, D. Synthesis of nanosized calcium hydroxyapatite particles by the catalytic decomposition of urea with urease, *Journal of Materials Research*, 2007, 22, 1156-1161, doi:10.1557/jmr.2007.0170.
- [19] Bayraktar, D.; Tas, A.C. Formation of hydroxyapatite precursors at 37C in urea- and enzyme urease-containing body fluids. *Journal of Materials Science Letters*, 2001, 20, 401-403, doi:10.1023/A:1010929825557.
- [20] Bayraktar, D.; Cu, A.; Tas, È. Chemical Preparation of Carbonated Calcium Hydroxyapatite Powders at 37 C in Urea-containing Synthetic Body Fluids. *Journal of*

*European Ceramic Society*, 1999, 19, 2573-2579.

- [21] Peng, X.; Chen, A.; Large-scale synthesis and characterization of TiO<sub>2</sub>-based nanostructures on Ti Substrates. *Advanced Functional Materials*, 2006, 16, 1355-1362, doi:10.1002/adfm.200500464.
- [22] Pasinli, A.; Yuksel, M.; Celik, E.; Sener, S.; Tas, A.C. A new approach in biomimetic synthesis of calcium phosphate coatings using lactic acid-Na lactate buffered body fluid solution. *Acta Biomaterialia*, 2010, 6, 2282-2288, doi:10.1016/j.actbio.2009.12.013.
- [23] Su, C.Y.; Zhou, Q.; Zou, C.H. Surface deposition on titania in a physiological solution with ultraviolet irradiation in situ and effect of heat treatment. *Coatings*, 2019, 9, 80, doi:10.3390/coatings9020080.
- [24] Muller, L.; Muller, F.A. Preparation of SBF with different HCO<sub>3</sub><sup>-</sup> content and its influence on the composition of biomimetic apatites. *Acta Biomaterialia*, 2006, 2, 181-189, doi: 10.1016/j.actbio.2005.11.001.